



**HAL**  
open science

# Design, Fabrication and Characterization of a Novel Piezoresistive Pressure Sensor for Blast Waves Monitoring

K Sanchez, Bilel Achour, J Riondet, L Anglade, M Carrera, Anthony Coustou, Aurélie Lecestre, Samuel Charlot, Hervé Aubert, M Lavayssière, et al.

► **To cite this version:**

K Sanchez, Bilel Achour, J Riondet, L Anglade, M Carrera, et al.. Design, Fabrication and Characterization of a Novel Piezoresistive Pressure Sensor for Blast Waves Monitoring. *SENSORDEVICES 2021, The Twelfth International Conference on Sensor Device Technologies and Applications*, Nov 2021, Athènes, Greece. hal-03545876

**HAL Id: hal-03545876**

**<https://hal.science/hal-03545876>**

Submitted on 29 May 2022

**HAL** is a multi-disciplinary open access archive for the deposit and dissemination of scientific research documents, whether they are published or not. The documents may come from teaching and research institutions in France or abroad, or from public or private research centers.

L'archive ouverte pluridisciplinaire **HAL**, est destinée au dépôt et à la diffusion de documents scientifiques de niveau recherche, publiés ou non, émanant des établissements d'enseignement et de recherche français ou étrangers, des laboratoires publics ou privés.

Copyright

# Design, Fabrication and Characterization of a Novel Piezoresistive Pressure Sensor for Blast Waves Monitoring

K. Sanchez, B. Achour, J. Riondet, L. Anglade,  
M. Carrera, A. Coustou, A. Lecestre, S. Charlot,  
H. Aubert, P. Pons  
CNRS-LAAS, Toulouse University  
Toulouse, France  
ksanchezba@laas.fr, bachour@laas.fr, jriondet@laas.fr,  
acoustou@laas.fr, alecestre@laas.fr, scharlot@laas.fr,  
haubert@laas.fr, ppons@laas.fr

M. Lavyssière, A. Lefrançois, J. Luc  
CEA-DAM  
Gramat, France  
maylis.lavyssiere@cea.fr, alexandre.lefrancois@cea.fr,  
jerome.luc@cea.fr,

**Abstract**— In several side-on configurations, the monitoring of blast wave requires sensor with very low response time ( $< 1 \mu\text{m}$ ). The sensing area of commercial sensors are too high to fulfill this specification. New transducers are focused on miniature membrane (diameter  $< 100 \mu\text{m}$ ) but with optical transduction which has the disadvantage of low integration for multiple transducers. In this communication, a miniature piezoresistive pressure transducer based on silicon membrane and silicon gauges is designed and fabricated. Shock tube characterizations of the sensor have shown promising dynamic behavior with a rise time of 30 ns and a response time lower than  $1 \mu\text{s}$  thanks to a membrane fundamental resonant frequency of 20 MHz. Undesirable mechanical effects leading to the response drift after  $1 \mu\text{s}$  were identified, probably due to holder deformation.

**Keywords** – shock wave ; air blast ; pressure sensor

## I. INTRODUCTION

Blast waves monitoring is required for many civilian and military applications, and especially for explosives characterization. In this case, and for supersonic shock wave, the side-on over-pressure (i.e., when the transducer surface is parallel to the flow velocity) reaches quasi-instantaneously ( $< 10 \text{ ns}$ ) a maximum  $P_{\text{max}}$  (from several bar to several ten of bar) and then decreases rapidly (typically a few hundred microseconds). In order to quantify accurately the effect of supersonic shock wave on systems, the precise knowledge of  $P_{\text{max}}$  is mandatory [1]. For several setup configurations (mass of explosive, distance between source and sensor), sensors with response time lower than  $1 \mu\text{s}$  are then required.

The pressure sensors available on the market, that specifically address pyrotechnic applications, used mainly piezoelectric transducers with ceramic thick disk [2]-[3] or polymer thin film [4]. The typical response time of such sensors is about several microseconds for side-on configuration. High response times are mainly due to the large diameter ( $> 900 \mu\text{m}$ ) of used piezoelectric layers in order to produce enough electrical charges. In order to reduce the response time, micro-membranes with a diameter lower than  $100 \mu\text{m}$  and based on optical transduction have been reported [5]-[6]-[7]-[8]. These sensors have good dynamic performances with frequency bandwidth higher than 10 MHz. But the optical transduction requires complex

technological steps and does not facilitate the high integration of multiple sensors.

Recently, we proposed a transducer using a miniature monocrystalline silicon membrane and silicon piezoresistive gauges [9]-[10]. The objective is to combine the advantage of miniature membrane (sensing diameter  $< 100 \mu\text{m}$ ) and the high integration of electronic transduction. In this paper, we report the design, fabrication and measurement results of this transducer, and we explore the unexpected and undesirable mechanical response observed beyond  $1 \mu\text{s}$ . The transducer design is presented in Section 2. The Section 3 is dedicated to the fabrication of the transducer. The static pressure response of the transducer is given in Section 4, thanks to COMSOL simulations. Finally, Section 5 describes the dynamic pressure response of the sensor using a shock tube.

## II. TRANSDUCER DESIGN

The topology of the transducer is displayed on Figure 1 and Figure 2.

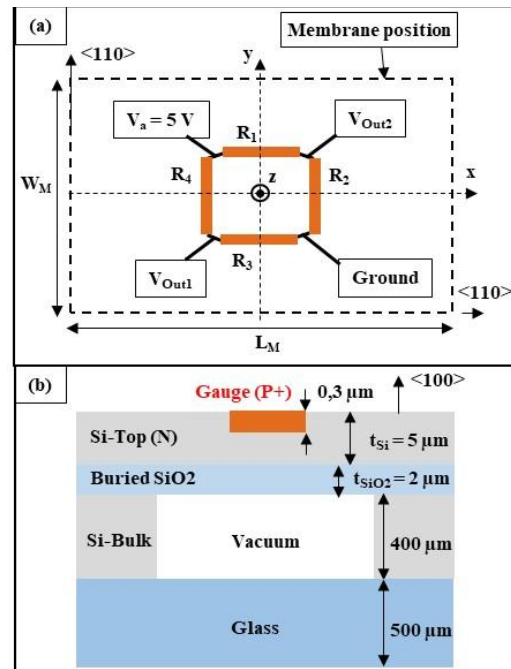


Figure 1. (a) Top view of the Wheatstone bridge reported on the membrane surface, (b) Cross sectional diagram of the transducer.

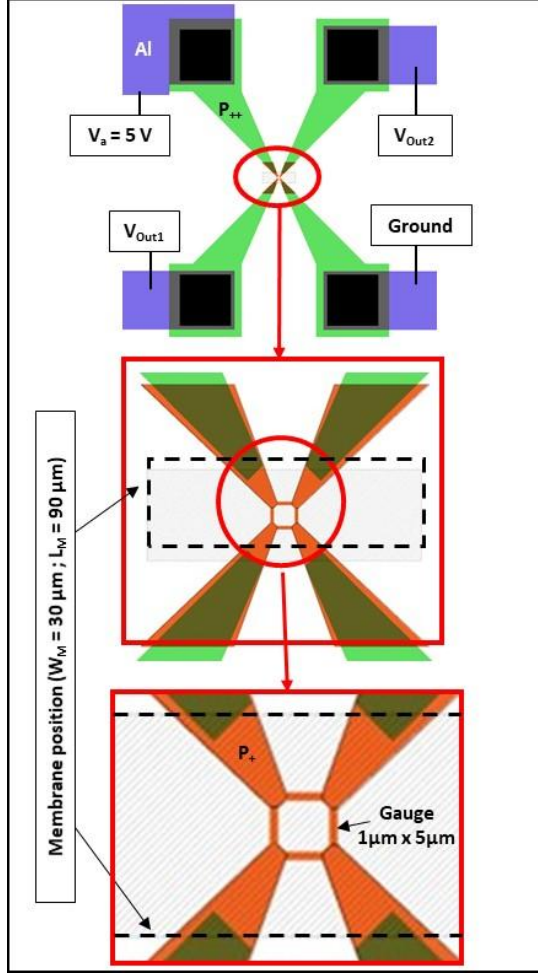


Figure 2. Top view of the mask used for the fabrication

A N-type monocrystalline  $5\mu\text{m}$ -thick silicon membrane is used for the mechanical transducer. This membrane is obtained by releasing the top layer of a Silicon-On-Insulator (SOI) substrate. Its shape is rectangular with targeted width  $W_M = 30\mu\text{m}$  and length  $L_M = 90\mu\text{m}$ . The electrical transducer is provided by P-type monocrystalline silicon gauges which are inserted at the center of the N-type silicon membrane and are distributed using the Wheatstone bridge configuration. The inter-isolation of the gauges is obtained from the reverse polarization of the P/N junction. The targeted gauges width is  $W_J = 1\mu\text{m}$  and length  $L_J = 5\mu\text{m}$ . The pressure is applied on the top side of the membrane and a reference cavity with vacuum is located at the bottom side of the membrane.

### III. TRANSDUCER FABRICATION

#### A. Technological fabrication steps

The transducer fabrication uses SOI wafers whose characteristics are given in Table 1. The transducer on its metallic holder is shown on Figure 3.

TABLE 1. SOI WAFERS CHARACTERISTICS PROVIDED BY THE SUPPLIER

Si-top	Orientation	(100)
	Type	N
	Doping level	$4.8 \cdot 10^{15}$ to $1.6 \cdot 10^{15}$ at/cm <sup>3</sup>
	Thickness	$(5.0 \pm 0.5)\mu\text{m}$
Buried SiO <sub>2</sub>	Thickness	$(2.0 \pm 0.1)\mu\text{m}$
Si Bulk	Orientation	(100)
	Thickness	$(400 \pm 15)\mu\text{m}$

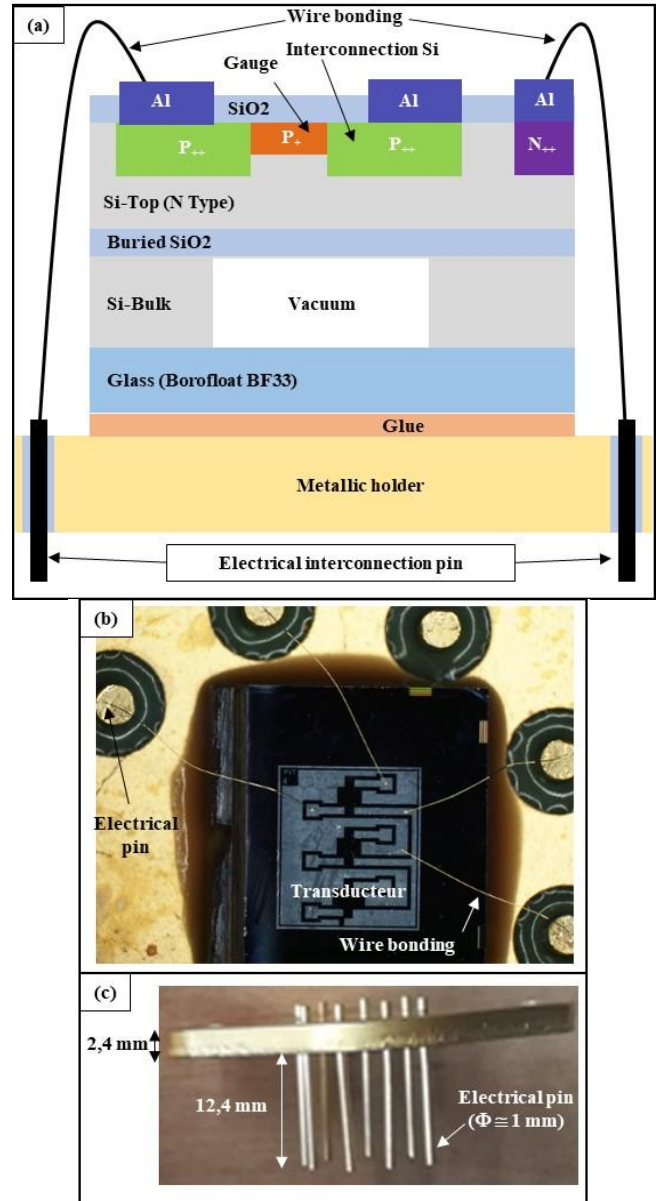


Figure 3. (a) Cross section diagram of the transducer on its metallic holder, (b) Top view of the transducer glued to the metallic holder, (c) View of TO3 metallic holder.

The main technological fabrication steps are described in the following.

The process starts with the growing of a 40nm-thick thermal silicon dioxide (SiO<sub>2</sub>). Boron and phosphorus implantation are then performed respectively for the low resistivity interconnections between gauges and metallic lines and for the electrical contact on SiN-top. Both implantations are done with the same parameters (Energy = 50 keV, Dose = 10<sup>16</sup> at/cm<sup>2</sup>). The activation annealing of dopants is then done during one hour at 1000°C.

The next step is dedicated to the gauge's fabrication with boron implantation (Energy = 20 keV, Dose = 5\*10<sup>14</sup> at/cm<sup>2</sup>). The activation annealing of dopants is done with rapid thermal annealing during one minute at 1000 °C, in order to hold the dopant close to the membrane surface where the stress is maximal and then maximize the transducer sensitivity. The surface concentration is of 3.5 10<sup>19</sup> at/cm<sup>3</sup> that is a good compromise between gauge sensitivity to strain and to temperature. The junction depth is of 0.3 μm.

Then the deposition of a 350nm-thick SiO<sub>2</sub> layer is performed at 300°C by Plasma Enhanced Chemical Vapor Deposition to provide enough electrical isolation between gauges and future metallic interconnections. After contact opening by liquid etching of SiO<sub>2</sub>, a 500nm-thick aluminum layer is deposited by thermal evaporation for metallic interconnections.

The silicon membrane is then released by Deep Reactive Ionic Etching (DRIE) of Si-bulk from back-side, up to the buried-SiO<sub>2</sub> stop layer.

After the anodic bonding of glass on silicon back side, the wafer is dicing and the die is gluing on a metallic holder. Wire bonding is finally performed between transducer pads and holder pin.

### B. Electrical characteristics of the fabricated gauges

The transducer resistance R<sub>Transd</sub> (between V<sub>out1</sub> and V<sub>out2</sub>) measured before the wafer dicing is of (2990 ± 100) Ω. This measurement result is slightly lower than the simulated one (3650Ω) obtained from COMSOL software : using mask dimension opening of W<sub>J</sub> = 1 μm and L<sub>J</sub> = 5 μm, the gauge resistance R<sub>J</sub> is of 1380 Ω. The difference with the transducer resistance R<sub>Transd</sub> is due to the access resistance (mainly the P<sub>+</sub> interconnection between the gauges and the P<sub>++</sub> interconnection).

As shown on Figure 4, the final dimensions of the fabricated gauge are impacted by the photoresist lateral under-etching d<sub>sur</sub> = (110 ± 40) nm (Figure 4-a) and also by the boron diffusion d<sub>lat</sub> (about 130nm) during annealing corresponding to a boron doping level of 1\*10<sup>19</sup> at/cm<sup>3</sup> (Figure 4**Erreur ! Source du renvoi introuvable.**-b). The final gauge width W<sub>Jf</sub> and length L<sub>Jf</sub> are respectively of 1.5 μm and 4.5 μm (equations (1) and (2)).

$$W_{Jf} = W_J + 2*d_{sur} + 2*d_{lat} \quad (1)$$

$$L_{Jf} = L_J - 2*d_{sur} - 2*d_{lat} \quad (2)$$

Using these dimensions (instead of the dimension of the mask opening), a very good agreement is obtained between the simulated transducer resistance R<sub>Transd</sub> (3110 Ω) and the measured resistance (2990 Ω ± 100 Ω).

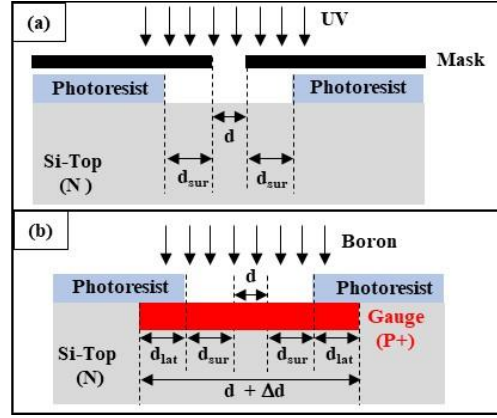


Figure 4. Cross section diagram of gauge showing lateral dimension increase due to the (a) Photoresist etching and (b) Boron diffusion.

### C. Membrane dimensions

As shown on Figure 5, the membrane width is higher than the mask opening. This originates in the lateral under-etching of the 40 μm-thick photoresist, the non-ideal vertical DRIE etching of silicon and finally the lateral under-etching of silicon related to the accumulation of chemical species, when the buried SiO<sub>2</sub> layer is reached.

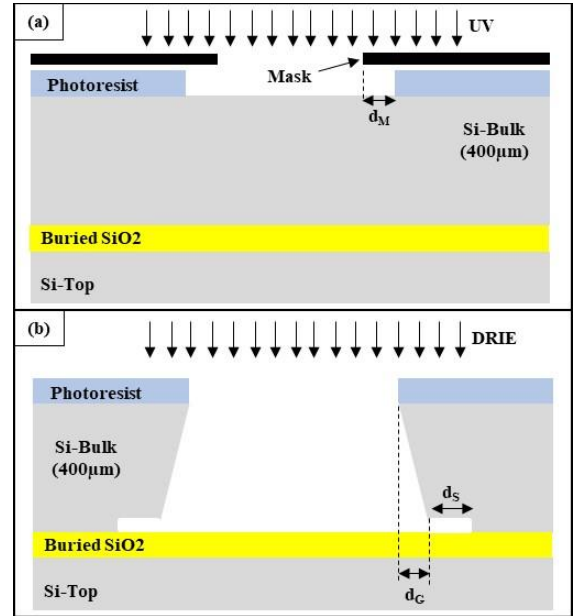


Figure 5. Cross section diagram of membrane showing lateral dimension increase due to the (a) Photoresist etching and (b) Si DRIE etching.

The dimensions of the fabricated membranes are measured on several samples using Focus Ion Beam (FIB) etching for cross section realization and Scanning Electron Microscopy (SEM) for dimensional measurements (Figure 6). The results obtained are given in Table 2.



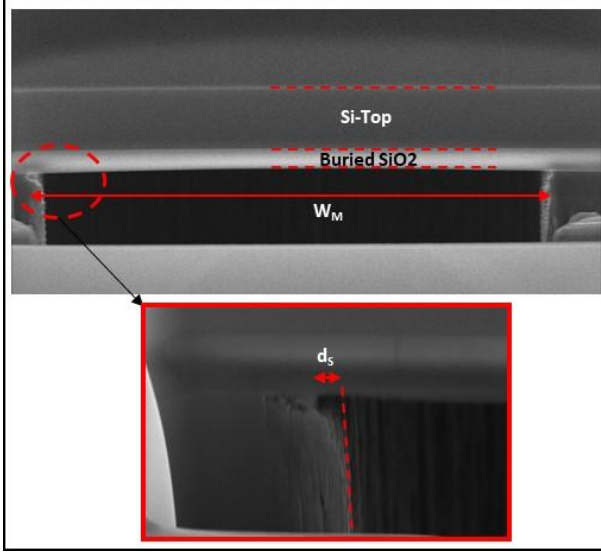


Figure 6. Cross section MEB photography after DRIE etching : a) full field of XX  $\mu\text{m}$  xYY  $\mu\text{m}$  and b) zoom on the right part.

TABLE 2. MEMBRANE DIMENSIONS MEASURED by SEM

Si-top thickness ( $\mu\text{m}$ )	$5.0 \pm 0.2$ to $5.7 \pm 0.2$
Buried SiO <sub>2</sub> thickness ( $\mu\text{m}$ )	$1.8 \pm 0.2$ to $2.0 \pm 0.2$
Membrane width ( $\mu\text{m}$ )	$39.5 \pm 0.2$ to $42.5 \pm 0.2$

The Si-top and buried SiO<sub>2</sub> measured thicknesses are in good agreement with the characteristics provided by the supplier (Table 1). The average membrane width is of 41  $\mu\text{m}$ , that is 37 % larger than the mask width, with a scattering of  $\pm 3.6$  %.

#### IV. SIMULATIONS RESULTS OF TRANSDUCER TO STATIC PRESSURE

COMSOL simulations were performed to predict the static transducer performances. The full design was considered (Figure 1 and Figure 2) with two membrane dimensions corresponding to the lowest and the highest mechanical stiffness given by the measured membrane dimensions (Table 2). The static pressure sensitivity and the fundamental mechanical resonant frequency are reported in Table 3.

TABLE 3. COMSOL SIMULATED TRANSDUCER PERFORMANCES

Case-1:  $t_{\text{Si}} = 4.8 \mu\text{m}$ ,  $t_{\text{SiO}_2} = 2 \mu\text{m}$ ,  $W_M = 43 \mu\text{m}$ ,  $L_M = 103 \mu\text{m}$   
 Case-2:  $t_{\text{Si}} = 5.9 \mu\text{m}$ ,  $t_{\text{SiO}_2} = 2 \mu\text{m}$ ,  $W_M = 39 \mu\text{m}$ ,  $L_M = 99 \mu\text{m}$

	Case 1	Case 2
Static pressure sensitivity $S_{\text{Transd}}$ ( $\mu\text{V}/\text{V}/\text{bar}$ )	209	138
Fundamental mechanical resonant frequency $F_0$ (MHz)	25.7	34.3

The simulated static pressure sensitivity is between 138  $\mu\text{V}/\text{V}/\text{bar}$  and 209  $\mu\text{V}/\text{V}/\text{bar}$ . The uncertainty on the transducer sensitivity is then of  $\pm 20.5$  %.

The simulated fundamental mechanical resonant frequency of the membrane is between 25.7 MHz and 34.3 MHz, corresponding to an uncertainty of  $\pm 14.3$  %.

#### V. SHOCK TUBE CHARACTERIZATION OF THE FABRICATED SENSOR

##### A. Setup description

The setup used for the dynamic pressure characterization of the sensor is illustrated on Figure 7.

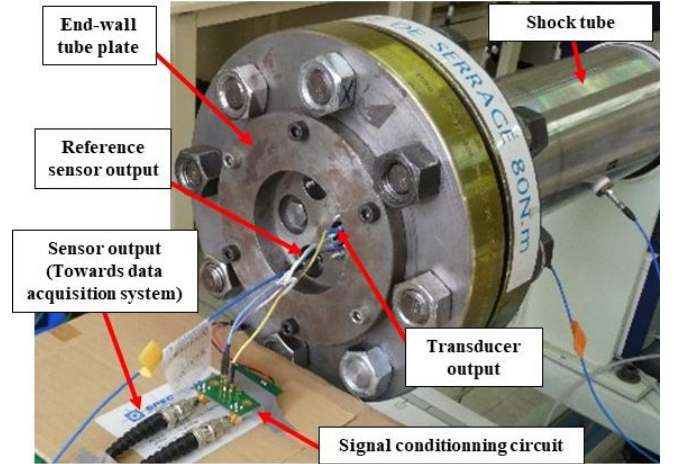


Figure 7. Experimental setup for dynamic pressure characterization.

A 2.7 m-length and 11cm inner-diameter metrological shock tube allows generating a pressure step with a rise time lower than 10 ns. The driver section is filled with nitrogen gas while the driven section is at atmospheric pressure. The diaphragm which separates the two sections is a standard nickel rupture disc that opens fully and responds within milliseconds to the applied overpressure. Its rupture creates a shock wave that propagates within the driven section until it reflects on the end-wall of the tube where the pressure is measured both by our transducer and a commercial reference sensor (PCB Piezotronics 134A24).

The transducer output is connected to a conditioning circuit via 10cm-length shielded wires. The static gain of this circuit is of 0.9 with a cut-of frequency of 35 MHz. The sampling frequency of the data acquisition system is of 100 MHz.

##### B. Sensor response to pressure step

The sensor response (at the output of the conditioning circuit) to a 10 bar pressure step is shown in Figure 8.

A typical damped oscillation is present in the first microsecond due to the excitation of the fundamental mechanical resonant mode of the membrane. From this measurement result, we can derive the transducer characteristics: a rise time of 30 ns, a response time lower than 1  $\mu\text{s}$  and a steady-state pressure sensitivity around 200  $\mu\text{V}/\text{V}/\text{bar}$ , assuming a gain of 0.9 from the conditioning circuit. This sensitivity is in good agreement with the predicted one.

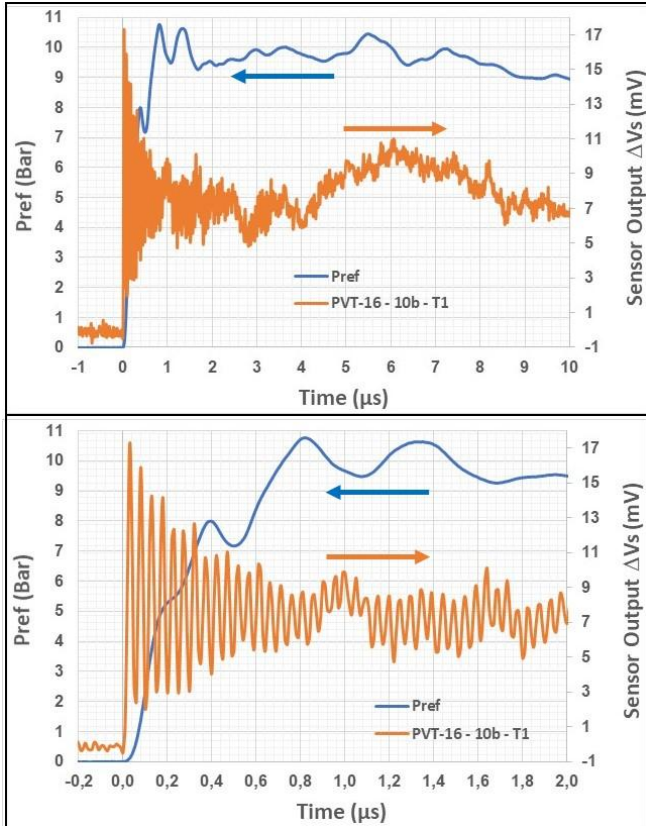


Figure 8. Sensor response to a 10 bar step pressure (orange line) and reference sensor (blue line)

The fundamental resonant frequency of 20.4 MHz is also in good agreement with the simulated one, as shown on Figure 9 describing the spectral analysis of the sensor response.

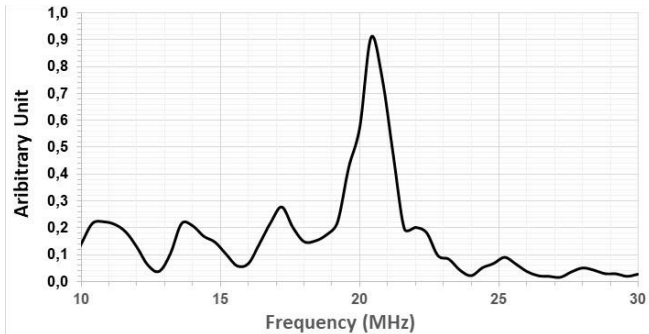


Figure 9. Spectral analysis of the sensor response

However, beyond 1  $\mu$ s, we observe that an unexpected drift appears. The next section is devoted to the interpretation of this drift.

### C. Analysis of the observed sensor drift

The sensor response to a 10 bar pressure step is shown in **Erreur! Source du renvoi introuvable.** using four different measurement configurations.

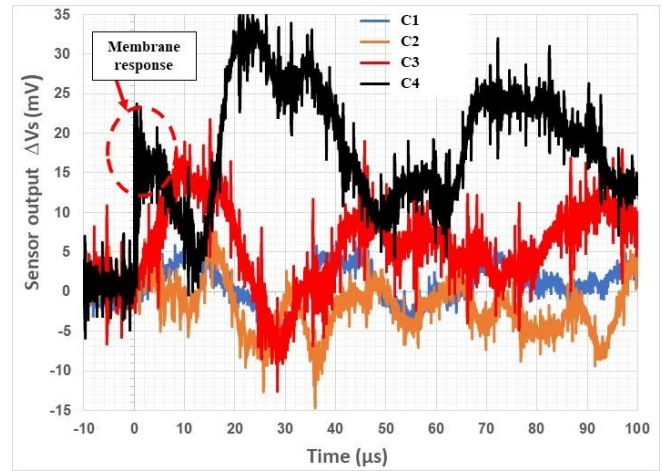


Figure 10. Sensor output with a 10 bar pressure step for different measurement configurations.

- Configuration C1: Without membrane - With Cover
- Configuration C2: Without membrane - Without Cover
- Configuration C3: With membrane - With Cover
- Configuration C4: With membrane - Without Cover

In configuration C1, the Si-Bulk is not removed below the gauges and a metallic cover is used to avoid direct shockwave effect (blue line). In this configuration, only indirect strain is applied on the gauges, without the membrane amplification, and a slow variation of the sensor response is observed, with an amplitude of  $\pm 5$ mV.

The same transducer is used in the configuration C2, but without the metallic cover (orange line). Compared with configuration C1, the sensor response is not significantly modified, but a higher amplitude ( $\pm 10$ mV) is observed due to the direct impact of the shock wave under the gauge and/or of the mechanical stiffening of the metallic holder by the metallic cover.

In the configuration C3, the response of a transducer with a membrane and a metallic cover is measured (red line). The large undesirable effect observed in the response (around 3 times of one recorded in the configuration C1) can be explained by the mechanical deformations of the metallic holder that is transmitted to the membrane and then amplified.

Finally, the same transducer used in the configuration C3 is measured in configuration C4, but without the metallic cover (black line). As expected, the membrane response is apparent in the first micro-seconds, and then the drift occurs.

## VI. CONCLUSIONS AND FUTURE WORKS

The characterization of supersonic shock wave produced by explosives requires sensor with response time lower than 1  $\mu$ s in order to quantify accurately the maximum overpressure in several side-on configuration. With sensing diameter greater than 900  $\mu$ m, the commercial sensors are not able to fulfill this specification.

Researches are focused on miniature membranes (diameter < 100  $\mu$ m) but with optical transduction that require complex technological steps and are not compatible with the integration of several transducers on the same chip.

We propose a pressure transducer based on a miniature silicon membrane and piezoresistive gauges in order to combine the advantage of miniature sensing area and microelectronic integration.

In this communication, a miniature piezoresistive pressure sensor was designed, fabricated and characterized with a shock tube. The transducer has a very low rise time (near to 30 ns) and a short response time (lower than 1  $\mu$ s) thanks to the high fundamental mechanical resonant mode of the membrane (near to 20 MHz).

Mechanical parasitic effects, that leads to large drift after few microseconds, were explored and identified. This effect is attributed to the metallic holder deformation under the passage of the shock wave. New packaging with higher mechanical stiffness will be designed in order to reduce these undesirable effects in the pressure response.

## ACKNOWLEDGMENT

This work was partially funded by Occitanie Region, France, through the COCNANO project and was supported by LAAS-CNRS micro and nanotechnologies platform members of the French RENATECH network.

## REFERENCES

- [1] L. Walter, "Air-blast and the Science of Dynamic Pressure Measurements", *Sound and Vibration*, Vol. 38, No 12, pp 10-17, Dec. 2004.
- [2] Piezotronics PCB [<https://www.pcb.com/sensors-for-test-measurement/pressure-transducers/blast-transducers>].
- [3] Kistler [<https://www.kistler.com/?type=669&fid=85810&model=document>].
- [4] Muller Instrument [<https://mueller-instruments.de/en/pressure-measurement/pressure-sensor-m/>].
- [5] N. Wu et al. "An ultra-fast fiber optic pressure sensor for blast event measurements", *Measurements Sciences and Technologies*, Vol. 23, No 5, April 2012, doi:10.1088/0957-0233/23/5/055102.
- [6] X. Zou, N. Wu, Y. Tian, C. Niezrecki, J. Chen, X. Wang, "Rapid miniature fiber optic pressure sensors for blast wave measurements", *Optics and lasers in Engineering*, Vol. 51, No 2, pp 134-139, Feb. 2013, doi : 10.1016/j.optlaseng.2012.09.001.
- [7] Z. Wang, G. Wen, Z. Wu, J. Yang, L. Chen, W. Liu, "Fiber optic method for obtaining the peak reflected pressure of shock wave", *Optic Express*, Vol. 28, No 12, June 2018, doi: 10.1364/OE.26.015199.
- [8] C. Chu, J. Wang, J. Qiu, "Miniature High-Frequency Response, High-Pressure-Range Dynamic Pressure Sensor Based on All-Silica Optical Fiber Fabry-Perot Cavity", *IEEE Sensor Journal*, Vol. 21, No 12, pp 13296-13304, June 2021, doi: 10.1109/JSEN.2021.3068456.
- [9] J. Riondet et al. "Design of air blast pressure sensors based on miniature silicon membrane and piezoresistive gauges", *Journal of Physics: Conference Series*, Vol. 922, Aug. 2017, doi: 10.1088/1742-6596/922/1/012019.
- [10] J. Veyrunes et al., "Transient response of miniaturized piezoresistive sensors for side-on pressure shockwave", *Proc. Design, Test, Integration & Packaging of MEMS/MOEMS*, 12-15 May 2019, Paris, France, doi: 10.1109/DTIP.2019.8752911.

